

# Spin–Orbit Coupling and Intersystem Crossing in Conjugated Polymers: A Configuration Interaction Description

D. Beljonne,<sup>\*,†,‡</sup> Z. Shuai,<sup>†</sup> G. Pourtois,<sup>†,‡</sup> and J. L. Bredas<sup>†,‡</sup>

Laboratory for Chemistry of Novel Materials, Center for Research in Molecular Electronics and Photonics, University of Mons-Hainaut, 20, Place du Parc, B-7000 Mons, Belgium, and Department of Chemistry, The University of Arizona, Tucson, Arizona 85721-0041

Received: January 17, 2001

Configuration–interaction calculations are performed to describe the singlet and triplet excited states of oligothiophene and oligo(phenylene ethynylene) conjugated chains. Intersystem crossing from the singlet to the triplet manifold is made possible by spin–orbit coupling, which leads to a mixing of the singlet ( $S_n$ ) and triplet ( $T_n$ ) wave functions. The electronic spin–orbit  $S_1$ – $T_i$  matrix elements, obtained from first-order perturbation theory, are used to compute the rates of intersystem crossing from the lowest singlet excited state,  $S_1$ , into low-lying triplet states,  $T_i$ . On the basis of these results, a general mechanism is proposed to describe the intersystem crossing process in conjugated oligomers and polymers. The roles of chain length, heavy-atom derivatization, and ring twists are evaluated.

## I. Introduction

Since the first report of electroluminescence in poly(paraphenylenevinylene), PPV, by the Cambridge group,<sup>1</sup> there has been an enormous amount of efforts dedicated to the development of light emitting diodes (LEDs) based on conjugated polymer materials. Despite the high performance achieved by current devices, the detailed mechanism for light generation in polymer-based LEDs is not fully established yet. One of the major issues in the field deals with the nature of the relaxed electronic excitations created upon charge injection and recombination. Two models are usually put forward when describing the electrooptical response of conjugated polymers:<sup>2</sup> (i) the semiconductor band model, where primary excitations correspond to band-to-band transitions and are therefore very much delocalized; and (ii) the excitonic model, where self-localization of the excitations takes place as a result of Coulomb interactions within the electron–hole pairs.

This issue bears strong impact on the working mechanisms of LEDs, namely on the role of triplet excitations as illustrated below. Triplets can form within the devices both upon recombination of the positive and negative charge carriers injected from the opposite electrodes and as a result of singlet–triplet intersystem crossing occurring once singlet species are generated in the organic layer. From simple spin statistics and assuming strongly bound excitons, the electroluminescence quantum yield,  $\eta(\text{EL})$ , is expected to be less than or equal to 25% of the photoluminescence quantum yield,  $\eta(\text{PL})$  (because the recombination of a pair of electron and hole leads to four microstates in total, with three triplets and one singlet).<sup>3</sup> Recent experimental data have, however, suggested  $\eta(\text{EL})/\eta(\text{PL})$  ratios as large as 50% in PPV-based devices.<sup>4–5</sup> These results can easily be accounted for in a semiconductor band model, because in this case the exchange energy is negligible and thermalized triplet excitons can contribute to luminescence (through activated

population migration from the triplet to the singlet manifold). Another possibility is that the exchange energy is large (exciton model), but that singlet and triplet excitons are formed with different cross sections. The latter scenario has been confirmed by correlated quantum-chemical calculations on PPV model conjugated chains.<sup>6</sup>

Once formed, the singlet excited species can decay either radiatively (light is emitted out of the device) or nonradiatively (thereby lowering the resulting luminescence quantum efficiency). A possible nonradiative decay route consists of an intersystem crossing (ISC) from the singlet to the triplet manifold, which is allowed by spin–orbit coupling (SOC) mixing the singlet and triplet wave functions. For oligothiophenes and polythiophenes in solution, intersystem crossing has been demonstrated to be the main nonradiative decay route of the singlet excitons;<sup>7–10</sup> note that in the solid state, interchain interactions can lead to luminescence quenching due to the formation of low-lying optically forbidden excited states.<sup>11,12</sup> The efficiency of the ISC route in thiophene-based conjugated materials has long been attributed to the “heavy-atom effect” associated with the sulfur atoms. In poly(paraphenylenevinylene) and derivatives, the existence of an intersystem crossing channel is supported by the appearance of a triplet–triplet transition band in photoinduced absorption spectra.<sup>13</sup> In the case of platinum-including poly-yne derivatives, the singlet-to-triplet crossing is so effective and the phosphorescence lifetime so short that only triplet emission is observed at low temperature.<sup>14</sup>

What is the exact origin for spin–orbit coupling in polythiophenes and typical hydrocarbon conjugated polymers? What is the most likely pathway for intersystem crossing in those materials? Can we design conjugated polymers with vanishing spin–orbit coupling in order to boost the quantum yield for singlet emission or, inversely, take advantage of triplet emission in conjugated structures with enhanced SOC? In this work, we try to provide some insight into these issues by studying oligomers of thiophene and of phenylene ethynylene, the latter being chosen as representatives for hydrocarbon conjugated systems. We first compute (i) the electronic excitation energies

\* Corresponding author.

† University of Mons-Hainaut.

‡ The University of Arizona.

from the ground state to the lowest singlet and triplet excited states of the oligomers; and (ii) the singlet–triplet spin–orbit coupling energies using first-order perturbation theory for selected molecules. Both pieces of information (excitation energies and SOC expectation values) are then inserted in the golden-rule expression for radiationless decay to estimate the ISC rates. The influence of twists along the conjugated path and the effects of extension of the conjugated bridge and its substitution with heavy atoms (such as chlorine and bromine) are investigated.

## II. Computation of the Spin–Orbit Coupling and Intersystem Crossing Rates

The ground-state geometric structures of all the conjugated oligomers considered in this work have been optimized at the Hartree–Fock semiempirical levels, using the AM1<sup>15</sup> technique in the case of oligo(phenylene ethynylene)s and the MNDO<sup>16</sup> method for the oligothiophenes (because it is our experience that AM1 performs less well in the case of sulfur-containing conjugated oligomers). Coplanar configurations have been adopted in all cases except when investigating the influence of ring twists.

The semiempirical intermediate neglect of differential overlap (INDO)<sup>17</sup> Hamiltonian is then combined with a single configuration interaction (SCI) scheme to describe the lowest singlet and triplet excited states. For the oligothiophenes, *d* orbitals on the sulfur atoms are included in the basis set. The Ohno–Klopman potential<sup>18</sup> is used to depict the electron–electron interactions. We find that this potential provides a more reliable estimate of the singlet–triplet,  $S_0$ – $T_i$ , energy difference than does the more conventional Mataga–Nishimoto potential.<sup>19</sup> We stress that higher order excitations have to be included in the CI expansion for a quantitative description of the transition energies.<sup>20</sup> Because here the emphasis is on trends rather than on numbers, the INDO (Ohno–Klopman)/SCI formalism, which provides a reasonable compromise between accuracy and computational demand, appears to be a useful approach.

Interaction between the spin and orbital motions of an electron (spin–orbit coupling) induces a mixing between singlet and triplet excitations. The spin–orbit Hamiltonian writes<sup>21</sup>

$$H_{so} = \alpha_{fs}^2 \sum_{\mu}^N \sum_i^n \frac{Z_{\mu}}{r_{i\mu}^3} \vec{L}_i \vec{S}_i \quad (1)$$

where  $\alpha_{fs}$  is the fine structure constant,  $Z_{\mu}$  is the effective nuclear charge for nucleus  $\mu$ , and  $L$  and  $S$  are the orbital and spin momenta, respectively. This Hamiltonian represents the coupling between the spin and orbital momenta of an electron  $i$ , through interaction with the nuclear field of nucleus  $\mu$ . Note that additional terms arising from electron–electron interactions should be included in  $H_{so}$  for a complete description of the spin–orbit interactions; these terms, usually assumed to be smaller, are neglected here.

The expectation value of the spin–orbit coupling can be calculated using first-order perturbation theory, with the spin–orbit interaction as the perturbation and the INDO/SCI unperturbed wave functions as the zero-order eigenvectors (with superscript 0):

$$\langle {}^1\Psi^0 | H_{so} | {}^3\Psi^0 \rangle = \alpha_{fs}^2 \sum_{\mu}^N \sum_i^n \left\langle \frac{Z_{\mu}}{r_{i\mu}^3} \psi^0 | \vec{L}_i | {}^3\psi^0 \right\rangle \times \left\langle \frac{1}{\sqrt{2}} (\alpha\beta - \beta\alpha) | \vec{S} | \frac{1}{\sqrt{2}} (\alpha\beta + \beta\alpha) \right\rangle \quad (2)$$

with  $\Psi^0(\psi^0)$  the INDO/SCI total (spatial) wave functions.

To compute the intersystem crossing rates,  $k^{IF}_{ISC}$ , between an initial singlet state I and a final triplet state F, we have used the golden-rule expression for radiationless transitions:<sup>22,23</sup>

$$k^{IF}_{ISC} = \frac{2\pi}{\hbar} \langle {}^1\Psi^0 | H_{so} | {}^3\Psi^0 \rangle^2 [\text{FCWD}] \quad (3)$$

where FCWD is the Franck–Condon weighted density of states, i.e., the density of vibrational states in the triplet times the Franck–Condon vibrational overlap. Note that eq 3 has been applied extensively for the treatment of electron-transfer (ET) reactions.<sup>22–24</sup> In the high-temperature limit, the FCWD term is given by<sup>24</sup>

$$\text{FCWD} = \frac{1}{\sqrt{4\pi\lambda RT}} \exp\left[-\frac{(\Delta E + \lambda)^2}{4\lambda RT}\right] \quad (4)$$

In eq 4,  $\lambda$  denotes the Marcus reorganization energy and  $\Delta E$  is the energy difference between the initial and final states, i.e., here the singlet–triplet energy splittings. In electron-transfer theory, the reorganization energy includes components from the vibration of the molecules (intramolecular reorganization energy) and from solvent reorientation around the molecules (solvent reorganization energy).<sup>22–24</sup> For intersystem crossing, solvent effects are expected to be small and  $\lambda$  corresponds to first approximation to the energy variation in the initial singlet excited state when switching from the singlet equilibrium geometry to the triplet equilibrium geometry.

## III. Singlet and Triplet Excitation Energies

Before going into the computation of the SO matrix elements and ISC rates, it is worth discussing the excitation energies computed for the lowest singlet and triplet excited states of the compounds considered in this work. As pointed out in the Introduction, the photophysical properties of oligothiophenes have been widely investigated using different spectroscopic techniques;<sup>7–10</sup> there is thus room for comparison between experiment and theory. Phenylene ethynylene oligomers are also attractive compounds, because numerous experimental data on the nature of the lowest singlet and triplet excitations have been reported on poly-yne structures including heavy atoms in the conjugated path.<sup>14,25</sup>

Figure 1 shows the evolution with inverse chain length of the INDO/SCI singlet–triplet,  $S_0$ – $T_1$ , and singlet–singlet,  $S_0$ – $S_1$  excitation energies in oligo(phenylene ethynylene)s and oligothiophenes (hereafter denoted as Ph<sub>*n*</sub> and Th<sub>*n*</sub>, with *n* equal to the number of aromatic rings, respectively). Note that all  $\pi/\pi^*$  molecular levels have been considered in the CI active space (the technique is therefore size-consistent for the  $\pi$  states we are interested in). The smaller chain-length dependence of the singlet–triplet energy difference, as compared to the singlet–singlet transition energy, is related to the more local character of the lowest triplet exciton with respect to the lowest singlet, as discussed previously.<sup>20,26</sup>

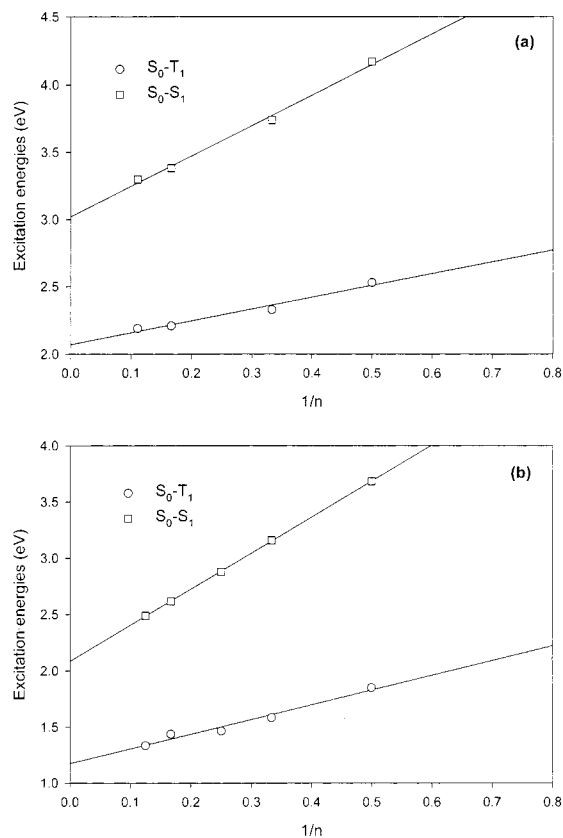


**Figure 1.** Evolution with inverse chain length,  $1/n$  (where  $n$  is the number of aromatic rings), of the INDO/SCI singlet–triplet,  $S_0-T_1$  (circles), and singlet–singlet,  $S_0-S_1$  (squares), excitation energies in (a) oligo(phenylene ethynylene)s and (b) oligothiophenes. Coplanar conformations are considered.

For oligothiophenes, the SCI excitation energies are found to be in reasonable agreement with those obtained at the more sophisticated multireference determinant MRD-CI level<sup>20</sup> (although SCI tends to underestimate the  $S_0-T_1$  energy separation) and with the results of recent spectroscopic and photoacoustic measurements.<sup>27</sup> From those measurements, the exchange energy ( $S_1-T_1$  energy difference) in the polymer (assuming infinite chain length) has been estimated to be on the order 0.6–0.9 eV, depending on the scheme used to extrapolate the experimental data. The SCI result is  $\sim 0.8$  eV and the MRD-CI calculations<sup>20</sup> yield  $\Delta E(S_1-T_1) \sim 0.6$  eV, i.e., both values lie within the experimental error bar. Note that these values for the exchange energy in polythiophene should be regarded as lower limits, because the conjugation length in actual polythiophene samples is finite and the singlet–triplet,  $S_1-T_1$ , energy separation is characterized by a strong chain-length dependence: the splitting is as large as 1.5 eV in short oligomers.<sup>20,27</sup>

In the case of oligo(phenylene ethynylene)s, extrapolation of the INDO/SCI computed excitation energies to infinite chains leads to an exchange energy close to 1 eV, i.e., slightly larger than the corresponding value in polythiophene. This is expected since the  $S_1-T_1$  energy separation increases with the degree of confinement of the excitations, which is larger in oligo(phenylene ethynylene)s due mainly to the presence of the strongly alternated triple bonds. To our knowledge, no experimental data are available for the triplet states in oligo(phenylene ethynylene)s. In a platinum-including poly(phenylenediethynylene), an exchange energy of  $\sim 1$  eV has been determined from a direct measurement of the phosphorescence spectrum,

allowed by the large spin–orbit coupling associated to the heavy platinum center.<sup>14</sup>

In both series of compounds, a rather large energy splitting between the lowest singlet,  $S_1$ , and triplet,  $T_1$ , excited states is thus obtained from the INDO/SCI calculations, in agreement with the available experimental data. Note that a similar value (0.9 eV) has recently been reported for a poly(paraphenylenevinylene) derivative.<sup>28</sup> Direct measurement of the phosphorescence emission from a ladder-type poly(paraphenylene) has located the lowest triplet state some 0.65 eV below the lowest singlet.<sup>29</sup> We stress that such large exchange energies are inconsistent with semiconductor band models and can be rationalized only within bound exciton theory; this also means that, in such materials, thermalized  $T_1$  triplet excitons do not contribute significantly to photoluminescence or electroluminescence at room temperature, because the thermal energy is much smaller than the activation energy (i.e.,  $kT \ll \Delta(S_1-T_1)$ ).

From eqs 3 and 4, we see that the intersystem crossing rate strongly depends on the overlap between the vibrational wave functions in the initial and final states. For an exothermic process (i.e.,  $\Delta E < 0$ , the final triplet state below the initial singlet state), the activation energy and the radiationless transition decay rate first raise with increasing energy separation (for  $\Delta E < \lambda$ ), peak at  $\Delta E = \lambda$ , and finally decrease with  $\Delta E$  for large excited-state splitting ( $|\Delta E| > \lambda$ , inverted region). For energy spacings on the order of one eV, the overlap factor between the singlet initial state and the triplet final state is vanishingly small; therefore, on the basis of such simple energy arguments, the  $S_1-T_1$  intersystem crossing pathway appears as an inefficient route for nonradiative decay of the singlet excitons in most conjugated materials.

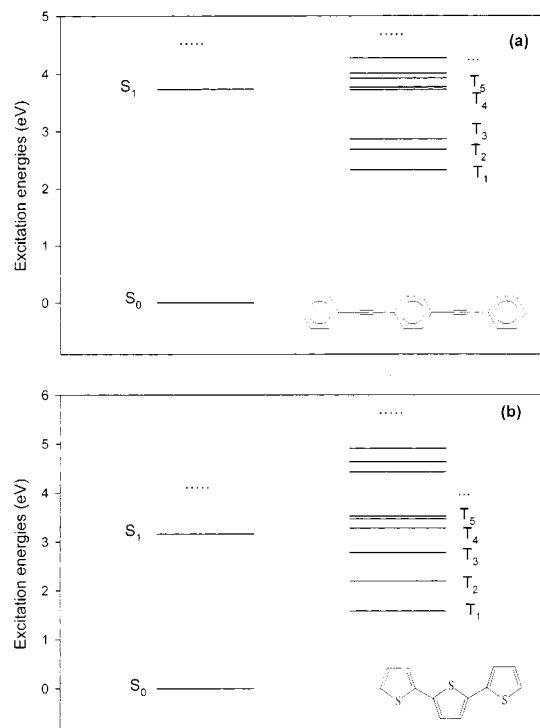
On the basis of the same arguments, channels for efficient intersystem crossing would be those involving quasi-degenerate pairs of singlet  $S_1$ /triplet  $T_i$  excited states, provided the  $S_1-T_i$  spin–orbit matrix element is sizable.<sup>30</sup> Note that if the final state is located at a higher energy than the initial state (i.e.,  $\Delta E > 0$ ), the barrier height for the activated intersystem crossing process increases with the singlet–triplet energy separation  $\Delta E$ . In terthiophene ( $Th_3$ ), the temperature dependence of the fluorescence quantum yield has been described on the basis of a model including contributions from two channels, a temperature-dependent pathway with an activation energy on the order of 0.05 eV (involving a triplet excited-state  $T_i$  close to  $S_1$ ) and a nearly temperature independent channel (involving other triplet states).<sup>8</sup> Quantum-chemical calculations, performed at the MRD-CI level, have confirmed this experimental observation and identified the triplet excited state closest to  $S_1$  as  $T_4$ .<sup>20</sup>

Figure 2 shows the energy diagram for the lowest singlet and triplet excited states of the planar  $Th_3$  and  $Ph_3$  molecules, as provided by the INDO/SCI scheme. In both cases, we find triplet states close in energy to  $S_1$ ; on the basis of simple energetic arguments, these are expected to contribute the most to the total intersystem crossing rate (small vibrational overlap and large activation energy reduce the contributions from low- and high-lying triplet states). To obtain a full picture, however, the spin–orbit couplings among the singlet and triplet excitations and the Franck–Condon overlap factors have to be quantified. This is done in the next two sections.

#### IV. Spin–Orbit Coupling

In order for the space part of integral (2) not to vanish, the direct product of the irreducible representations of  $^1\psi^0$  and  $^3\psi^0$  must contain the irreducible representation to which one or more of the three components of  $L$  ( $L_x$ ,  $L_y$ , and  $L_z$ ) belongs; these are





**Figure 2.** Energy diagram for the lowest singlet and triplet excited states in (a) the phenylene ethynylene trimer, Ph<sub>3</sub>, and (b) the thiophene trimer, Th<sub>3</sub>. Coplanar conformations are considered.

**TABLE 1: Symmetry Selection Rules for Intersystem Crossing**

symmetry group	initial state symmetry	final state symmetry	polarization
$D_{2h}$	$B_{3u}$	$B_{3u}$	forbidden
	$B_{2u}$	$B_{2u}$	forbidden
$C_{2h}$	$B_{2u}$	$B_{1u}$	out-of-plane
	$B_u$	$B_u$	out-of-plane
	$A_g$	$A_g$	out-of-plane
$C_{2v}$	$A_g$	$B_u$	forbidden
	$B_1$	$B_1$	forbidden
	$A_1$	$A_1$	forbidden
$C_2$	$A_1$	$B_1$	out-of-plane
	$B$	$B$	in-plane (short axis)
	$A$	$A$	in-plane (short axis)
	$A$	$B$	in-plane (long axis)

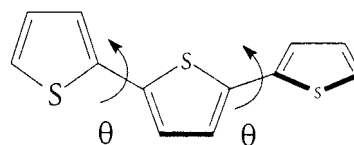
the symmetry selection rules for spin–orbit coupling. In planar conformations, the oligo(phenylene ethynylene)s have  $D_{2h}$  symmetry, whereas the oligothiophenes have either  $C_{2h}$  (for an even number of aromatic rings) or  $C_{2v}$  (for an odd number of aromatic rings) symmetry. Inspection of the character tables for these point groups indicates that, depending on the symmetry of the initial and final excited states (see Table 1), ISC between  $\pi$ – $\pi^*$  excited states is forbidden, except in the out-of-plane direction (and hence negligible for planar compounds). Of course, as for optical transitions, the selection rules for spin–orbit mixing can be somewhat relaxed through vibronic couplings, though this second-order effect is expected to be weak in most cases.<sup>21</sup> As both ISC and phosphorescence involve the SOC expectation values, these processes are predicted, from simple symmetry arguments, to occur with a very small probability in highly symmetrical, planar, conjugated structures (even if the conjugated backbone includes heavy atoms).

If we now impose a twist angle along the conjugated path of the molecules, the symmetry is lowered to  $C_2$  (or lower symmetry), for which spin–orbit coupling is allowed either along the  $C_2$  rotation axis (short axis of the molecule) for excited

states belonging to the same irreducible representation or along the main chain axis for excited states belonging to different representations (Table 1). Therefore, it is likely that rotation of the aromatic rings along the conjugated segments will considerably enhance the spin–orbit couplings and hence the transition probabilities for intersystem crossing and triplet light emission. Note, however, that geometry relaxation in the excited state is expected to lead to more planar conformations, as a result of the increased quinoid character within the thiophene<sup>9</sup> or phenylene rings. Two scenarios can then be invoked to explain efficient ISC: either torsional relaxation to a fully planar conformation is impeded by steric hindrance or the process takes place from an unrelaxed nonplanar singlet excited state conformation.

In the case of polythiophenes, the conformations adopted by the chains depend on the size and nature of the substituent groups in positions. Recent experiments by Theander et al.<sup>31</sup> have demonstrated a *decrease* in fluorescence quantum yield in solution when grafting bulky groups on the polythiophene chains, resulting mainly from more efficient nonradiative decay channels; similar findings have been reported by Lanzani et al.<sup>32</sup> From the above considerations, these data can be interpreted within the first scenario as resulting from a faster intersystem crossing channel due to the enhanced SOC in those conjugated chains that likely keeps a nonplanar conformation in the excited state. (Note that internal conversion is not a likely explanation for this observation, because twisted structures are characterized by higher excitation energies and the IC rate decreases with increasing energy separation.) Molecular disorder thus appears as a key parameter in the control of the nonradiative decay rates and the singlet emission quantum efficiencies. In that respect, the very high photoluminescence efficiency of ladder-type poly-(paraphenylene)s (LPPP) in solution (on the order of 80%<sup>33</sup>) appears to be related to the particularly low intrachain disorder in this polymer. Using femtosecond time-resolved spectroscopy, Rentsch and co-workers have demonstrated that the high generation of triplets in Th<sub>2</sub> and Th<sub>3</sub> arises because of a very efficient ISC channel involving the unrelaxed, nonplanar singlet  $S_1$  excited state and a closely lying triplet state.<sup>10</sup> This supports the second scenario described above as a possible mechanism for the intersystem crossing process in unsubstituted oligothiophenes.

In our approach, the SOC expectation values have been computed for a series of model compounds, where we impose a twist of the aromatic rings along the conjugation path following an helical conformation. This is depicted below for the thiophene trimer ( $\theta$  is the interannular twist angle, taken here as a free parameter): Since internal conversion is usually



a very fast process (the IC decay rates are on the order of  $10^{12}$ – $10^{13}$  s<sup>-1</sup>), intersystem crossing is likely to take place from the lowest singlet excited state in its relaxed geometry. Note, however that, upon excitation in the high-energy domain of the optical spectrum of polythiophene (around 6 eV), a new efficient channel for intersystem crossing opens up, which involves high-lying singlet and triplet excited states most likely localized on the thiophene aromatic rings.<sup>34</sup> Here, all spin–orbit coupling elements have been computed with the lowest singlet excited state,  $S_1$ , as the initial state. Note that all valence molecular

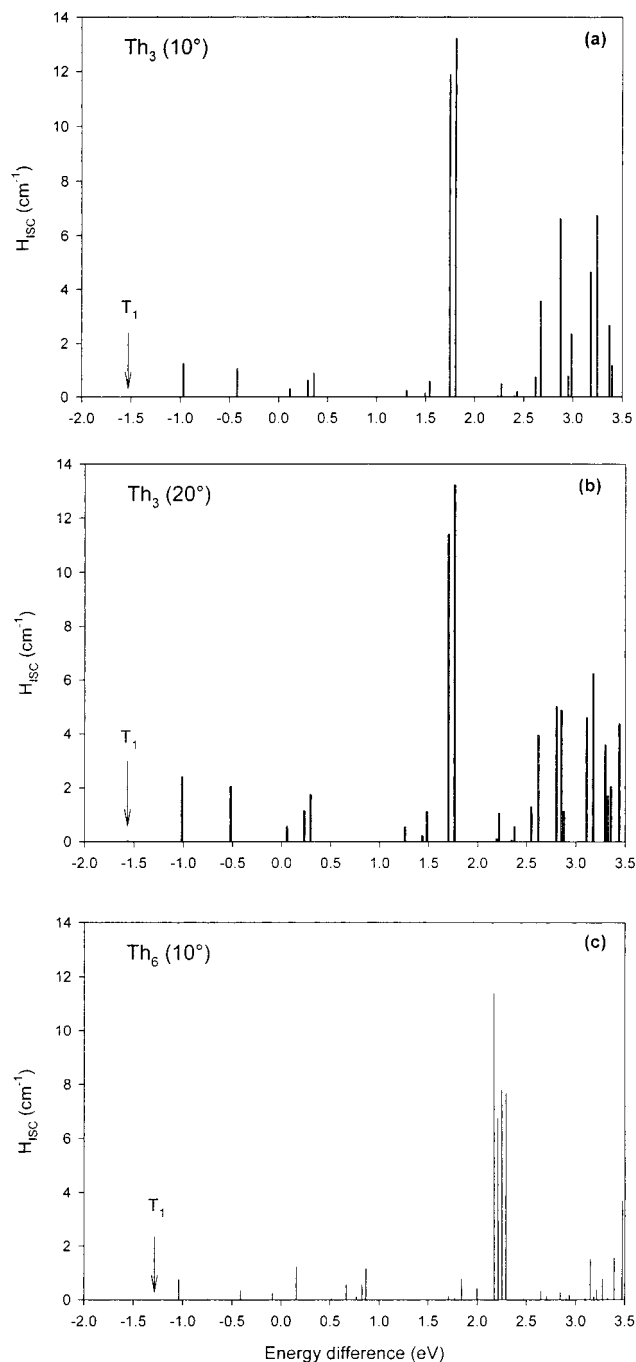


**Figure 3.** Spin–orbit coupling matrix elements (in  $\text{cm}^{-1}$ ) between the  $S_1$  singlet excited state and the lower-lying triplet  $T_i$  excited states of (a) the thiophene trimer,  $\text{Th}_3$ , with ring twists of  $10^\circ$ ; (b) the thiophene trimer,  $\text{Th}_3$ , with ring twists of  $20^\circ$ ; and (c) the thiophene hexamer,  $\text{Th}_6$ , with ring twists of  $10^\circ$ . The abscissa is the energy difference (in eV) between the final triplet excited state ( $T_i$ ) and the initial singlet excited state ( $S_1$ ).

orbitals have been included in the CI active space. For the compounds investigated here, the spin–orbit expectation values are on the order 1–40  $\text{cm}^{-1}$ , which are typical values for organics.<sup>21</sup> The results are displayed in Figures 3–5 (where the  $x$ -axis corresponds to the energy difference between the initial  $S_1$  singlet excited state and the final  $T_i$  triplet state).

Our main findings are:

(i) For all compounds investigated, the spin–orbit coupling between the  $S_1$  and  $T_1$  excited states is vanishingly small. This has to be related to the fact that the  $T_1$  triplet excited state is described in terms of a few electronic configurations involving

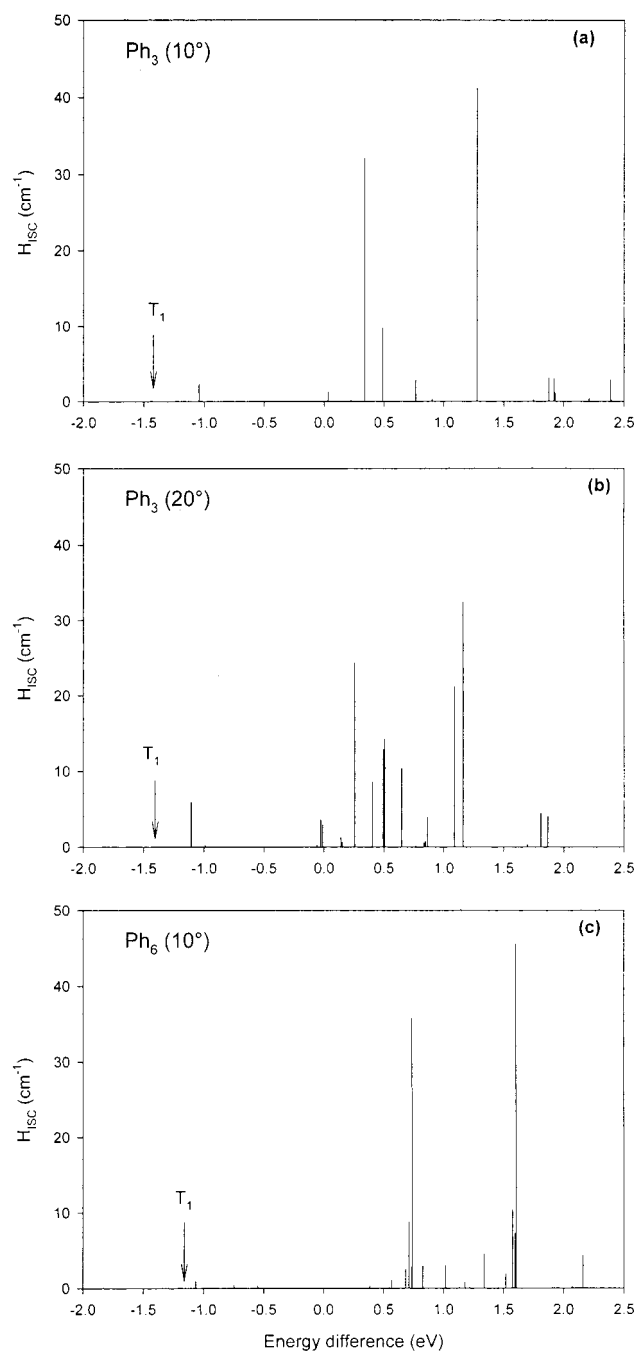


**Figure 4.** Spin–orbit coupling matrix elements (in  $\text{cm}^{-1}$ ) between the  $S_1$  singlet excited state and the lower-lying triplet  $T_i$  excited states of (a) the phenylene ethynylene trimer,  $\text{Ph}_3$ , with ring twists of  $10^\circ$ ; (b) the phenylene ethynylene trimer,  $\text{Ph}_3$ , with ring twists of  $20^\circ$ ; and (c) the phenylene ethynylene hexamer,  $\text{Ph}_6$ , with ring twists of  $10^\circ$ . The abscissa is the energy difference (in eV) between the final triplet excited state ( $T_i$ ) and the initial singlet excited state ( $S_1$ ).

the frontier molecular orbitals with strong  $\pi$  character (mainly the HOMO to LUMO and HOMO-1 to LUMO + 1 excitations). As discussed previously, spin–orbit interactions between  $\pi$ – $\pi^*$  electronic transitions is expected to be very weak.<sup>35</sup>

(ii) In the oligothiophenes (Figure 3), large SO couplings are calculated for triplet excited states located 1.5–2.5 eV above the lowest singlet. From the analysis of the wave functions, these triplet excitations can be classified as quasi-pure  $\pi$ – $\sigma^*$  excitations, which are well-known to lead to efficient intersystem crossing in heterocyclic compounds.<sup>21,36</sup> Most importantly, triplet excited states located in the vicinity of  $S_1$  are found to

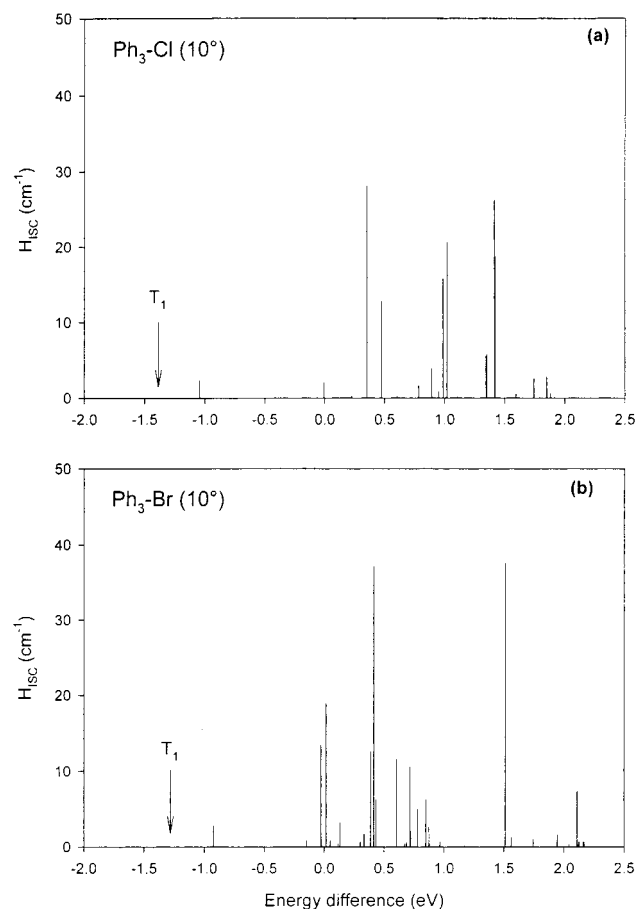


**Figure 5.** Spin-orbit coupling matrix elements (in  $\text{cm}^{-1}$ ) between the  $S_1$  singlet excited state and the lower-lying triplet  $T_i$  excited states of (a) the chloro-substituted phenylene ethynylene trimer,  $\text{Ph}_3\text{-Cl}$ , with ring twists of  $10^\circ$  and (b) the bromo-substituted phenylene ethynylene trimer,  $\text{Ph}_3\text{-Br}$ , with ring twists of  $10^\circ$ . The halogen atoms are grafted on the phenylene rings in (2,5) positions. The abscissa is the energy difference (in eV) between the final triplet excited state ( $T_i$ ) and the initial singlet excited state ( $S_1$ ).

display sizable spin-orbit interaction with  $S_1$ ; although those electronic excitations are mainly of  $\pi\text{-}\pi^*$  nature, they also involve molecular orbitals with some  $\sigma$ -character (due to  $\sigma\text{-}\pi$  mixing) and large contributions on the sulfur atoms.

(iii) It is quite remarkable that observations (i) and (ii) also apply in the case of oligo(phenylene ethynylene)s, Figure 4. Here, however, the large peaks in the SOC values are due to triplet wave functions with large contributions arising from the perpendicular  $\pi$  system of the ethynylene triple bonds.

(iv) When focusing on the triplet excited states located in the vicinity or below  $S_1$ , we note that the spin-orbit expectation values increase when raising the twist angle between adjacent rings (which is expected) but *decrease* with increasing chain length. We rationalize the latter feature by the larger energetic separation between the  $\pi$  and  $\sigma$  electronic structures in the more extended compounds, which reduces the  $\sigma\text{-}\pi$  mixing and hence the spin-orbit interactions. This has important consequences on the chain-length evolution of the ISC rates, as discussed in the next section.

(v) Finally, because the spin-orbit Hamiltonian is highly sensitive to the atomic number  $Z$  (eq 1), substitution of the conjugated chains with heavy-atom-containing groups should lead to a large enhancement of the SOC expectation values. As shown in Figure 5, we find that derivatization of the  $\text{Ph}_3$  molecule with chlorine and especially bromine induces a substantial increase in the spin-orbit interactions for transitions

from  $S_1$  to close-lying triplet excited states, because these triplet states have significant contributions on the halogen atoms.

At this stage, we can already propose possible pathways for the intersystem crossing processes in conjugated chains. The direct  $S_1\text{-}T_1$  crossing route can be discarded because it is characterized by both a large energy splitting (hence a small Franck-Condon overlap) and a weak spin-orbit coupling. High-lying triplet states that present the largest spin-orbit couplings to  $S_1$  could be invoked, but activation energies larger than 0.5 eV lead to negligible FCWD in eq 4. Intersystem crossings from  $S_1$  to some closely lying  $T_i$  triplet states, characterized by sizable SOC, have therefore the greatest probability of occurring.

## V. Intersystem Crossing Rates

To quantify the last statement, we have inserted the expectation values for the spin-orbit operator into eq 3 to compute the intersystem crossing rates at room temperature ( $T = 298$  K). AM1/CI geometry optimizations on the lowest singlet and triplet excited states of  $\text{Th}_3$  provide us with estimates of the reorganization energies,  $\lambda$ . We find that the typical reorganization energy changes associated with geometrical relaxations when switching from the equilibrium geometry of the initial singlet state,  $S_1$ , to that of the final triplet state,  $T_i$ , (or vice-versa) are on the order 0.1–0.3 eV depending on the singlet-triplet pathway. These results are consistent with the upper limit for  $\lambda$  (0.3 eV) used by Burin and Ratner in their investigation of the spin effects on the luminescence yield of organic LEDs.<sup>30</sup>

The contributions to ISC in the terthiophene molecule (with a twist angle of  $20^\circ$ ) are shown for values of  $\lambda$  ranging from 0.15 to 0.4 eV in Figure 6. The most striking feature is that only two channels contribute significantly to the intersystem crossing: an exothermic pathway involving a triplet excited state ( $T_3$ ) located  $\sim 0.5$  eV below the lowest singlet state ( $S_1$ ) and an endothermic channel corresponding to a radiationless transition from  $S_1$  to a triplet state lying slightly above ( $T_4$ ). Contributions of all other channels (including the  $S_1\text{-}T_1$  pathway) vanish mainly because of the FCWD factor in eq 3. The existence of a two-channel process is consistent with recent femtosecond time-resolved experimental investigations<sup>10</sup> and earlier temperature-dependent fluorescence quantum yield measurements<sup>8</sup> on terthiophene.

From Figure 6, we see that the relative contributions arising from the two different channels get reversed when increasing the reorganization energy: while the  $S_1$  to  $T_4$  channel dominates for low  $\lambda$ , it becomes negligible for large  $\lambda$  values. In fact, for those excited states, we are in the intermediate coupling regime of radiationless theory ( $\Delta E \sim \lambda$ ). Because the exponential in eq 4 passes through a maximum (equal to 1) when  $|\Delta E| = \lambda$ , the Franck-Condon overlap and subsequently the intersystem crossing rate is highly sensitive to the relative location of the excited states and the actual choice for the reorganization energy. Experimentally, it seems that the two channels contribute more or less equivalently to the total intersystem crossing rate.<sup>8</sup>

We have applied the same methodology to calculate the ISC rates of a series of model compounds. As is the case for  $\text{Th}_3$ , a few number of ISC routes (two in most cases) have been identified in those molecules. The results, obtained by summing over all final triplet states in eq 3, are presented in Table 2 for three representative values of  $\lambda$ . We stress that the various approximations considered in the formalism used here (for excitation energies, SOC expectation values and Franck-Condon overlap) do not allow quantitative predictions of ISC rates. For instance, the radiationless transition rates obtained

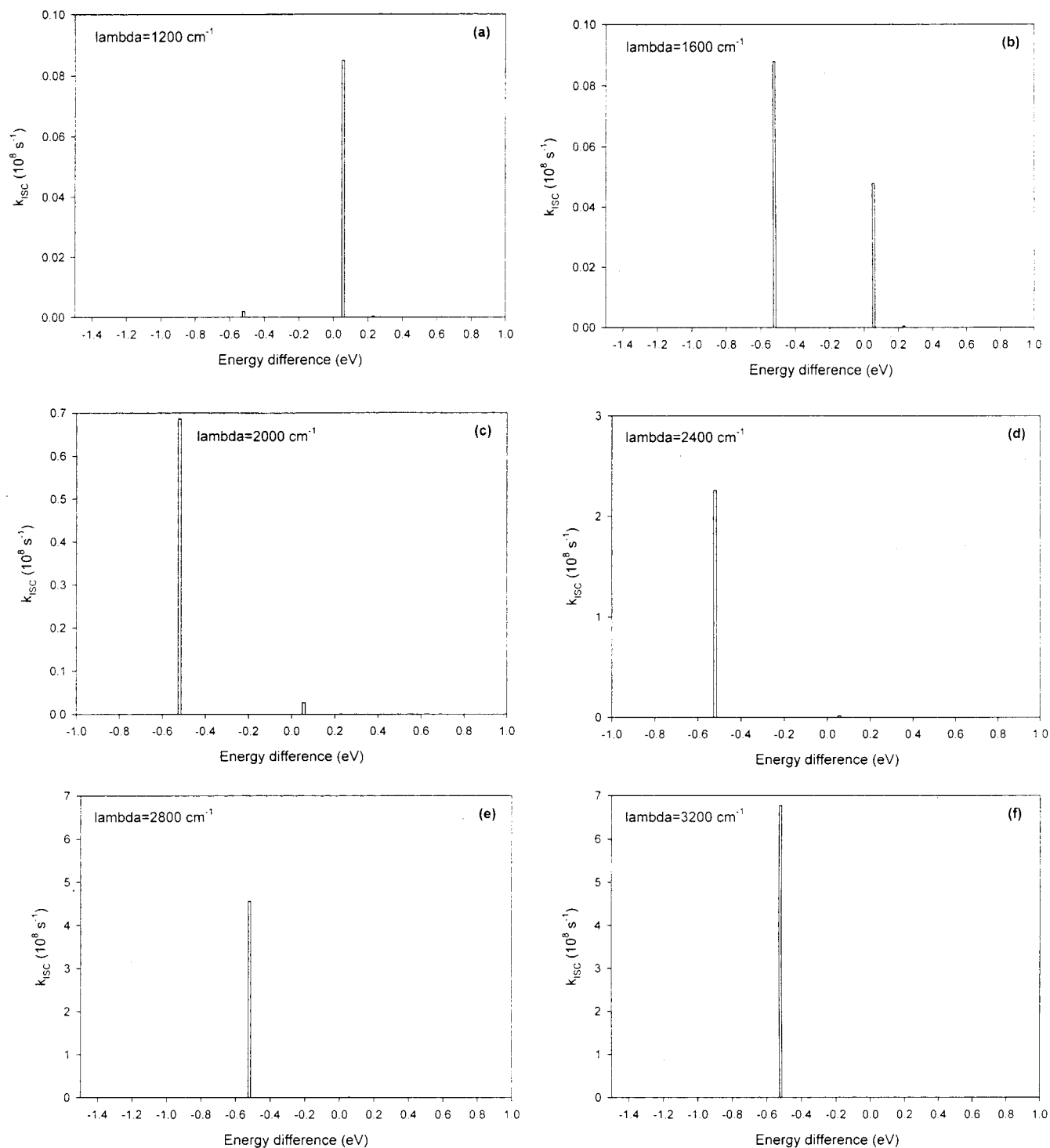


**Figure 6.** Calculated intersystem crossing rates (in  $10^8 \text{ s}^{-1}$ ) between the  $S_1$  singlet excited state and the lower-lying triplet  $T_1$  excited states of the thiophene trimer,  $\text{Th}_3$  (with ring twists of  $20^\circ$ ) at  $T = 298 \text{ K}$  for different values of the reorganization energy,  $\lambda$ : (a)  $\lambda = 1200 \text{ cm}^{-1}$ ; (b)  $\lambda = 1600 \text{ cm}^{-1}$ ; (c)  $\lambda = 2000 \text{ cm}^{-1}$ ; (d)  $\lambda = 2400 \text{ cm}^{-1}$ ; (e)  $\lambda = 2800 \text{ cm}^{-1}$ ; and (f)  $\lambda = 3200 \text{ cm}^{-1}$ . The abscissa is the energy difference between the final triplet excited state ( $T_1$ ) and the initial singlet excited state ( $S_1$ ). Note the major differences in the vertical scales.

for the oligothiophenes are about 1 order of magnitude smaller than the experimental values.<sup>8,9,37</sup> We believe, however, that the general description of the ISC mechanisms provided by our theoretical approach and the trends in the ISC rates observed upon substitution or elongation of the conjugated segment are valid.

The quantum-chemical calculations indicate a decrease with chain length of the intersystem crossing rates in oligothiophenes, which is consistent with a number of experimental data.<sup>9,37</sup> A similar evolution is obtained in the case of oligo(phenylene

ethynylene)s. In both cases, the decrease in  $k^{ISC}$  with the number of aromatic rings is mainly related to an overall lowering of the spin–orbit expectation values (as discussed in the previous section) but also, to a smaller extent, to an increase in energy barrier for the endothermic channel. For the oligothiophenes series, the  $S_1$  to  $T_4$  energy separation raises from  $\sim 0.05 \text{ eV}$  in the thiophene trimer to  $\sim 0.2 \text{ eV}$  in the thiophene hexamer (there is no significant endothermic contribution to ISC for the dimer). Note that similar results were obtained at the MRD-CI level<sup>20</sup> and agree well with the corresponding experimental values.<sup>8,10</sup>

**TABLE 2: Calculated Intersystem Crossing Rates (in  $10^8$   $s^{-1}$ ) at Room Temperature ( $T = 298$  K) for the Different Compounds Considered in This Work<sup>a</sup>**

compound	$\lambda = 1200$ $cm^{-1}$	$\lambda = 2000$ $cm^{-1}$	$\lambda = 2400$ $cm^{-1}$
Th <sub>2</sub> ( $\theta = 15^\circ$ )	7.2	4.4	1.9
Th <sub>2</sub> ( $\theta = 30^\circ$ )	8.8	18.	13
Th <sub>3</sub> ( $\theta = 10^\circ$ )	0.03	0.96	2.3
Th <sub>3</sub> ( $\theta = 20^\circ$ )	0.09	0.71	4.6
Th <sub>6</sub> ( $\theta = 10^\circ$ )	0.20	0.18	0.26
Ph <sub>3</sub> ( $\theta = 10^\circ$ )	0.68	0.21	0.07
Ph <sub>3</sub> ( $\theta = 20^\circ$ )	28	8.6	2.8
Ph <sub>3</sub> -Cl ( $\theta = 10^\circ$ )	4.2	1.3	0.45
Ph <sub>3</sub> -Br ( $\theta = 10^\circ$ )	503	151	49
Ph <sub>6</sub> ( $\theta = 10^\circ$ )	$10^{-5}$	0.01	0.09

<sup>a</sup> $\lambda$  is the reorganization energy;  $\theta$  is the interannular twist angle.

At the same time, the singlet–singlet,  $S_1$ – $S_0$ , radiative decay rate,  $k_R$ , calculated on the basis of the INDO/SCI excitation energies and oscillator strengths, increases slightly from  $\sim 2.5$  to  $\sim 5 \times 10^8$   $s^{-1}$  when passing from Th<sub>2</sub> to Th<sub>6</sub>; these values are consistent with the results of time-resolved fluorescence studies on oligothiophenes in solution, indicating an increase in  $k_R$  from Th<sub>3</sub> ( $\sim 3 \times 10^8$   $s^{-1}$ ) to Th<sub>6</sub> ( $\sim 5 \times 10^8$   $s^{-1}$ ).<sup>37</sup> As a consequence, while intersystem crossing competes in a very efficient way with singlet light emission in short oligomers, the radiative route for the singlet exciton decay dominates in long chains, leading to the overall increase in fluorescence quantum yields with the number of repeating units.<sup>9,37</sup> It is worth stressing that intermolecular interactions, which usually lead to a strong quenching of the luminescence in the solid state (for H-aggregates),<sup>11–12</sup> have also been shown to be minimized in highly extended conjugated structures;<sup>38</sup> these therefore appear as attractive materials for use as emissive component in LEDs.

Substitution of the phenylene units with chlorine and bromine induces a marked enhancement of the intersystem crossing rate in Ph<sub>3</sub>, as expected from the “heavy-atom” argument. We stress that this exaltation occurs because the halogen atoms contribute significantly to the wave functions of the low-lying electronic excited states and, therefore, the conditions of large spin–orbit coupling and significant vibrational overlap are simultaneously fulfilled.

Finally, we would like to comment on the possibility for observation of phosphorescence (i.e., triplet emission) in organic conjugated polymers. For the different compounds studied here, we have estimated phosphorescence radiative lifetimes in the range 0.2–2 s. Taking into account the very long natural lifetime of the triplet excitons in organics, their decay is expected to be in most cases entirely dominated by faster radiationless transitions such as quenching by a defect or impurity (such as molecular oxygen) in disordered conjugated polymers. Observation of phosphorescence in a conjugated polymer thus requires a high degree of order and a very low concentration of impurities or defects, conditions which are usually very hard to achieve. The first demonstration of phosphorescence in an hydrocarbon conjugated polymer was reported in a ladder-type poly(paraphenylene) conjugated polymer.<sup>29</sup>

## VI. Synopsis

Correlated quantum-chemical calculations have been performed to describe the singlet and triplet electronic excitations in oligothiophenes and oligo(phenylene ethynylene)s. By extrapolation of the transition energies obtained for oligomers of increasing size, we predict exchange energies on the order of one eV for the lowest excited state in the polymer chains. Such a large energy separation is expected to prevent any significant

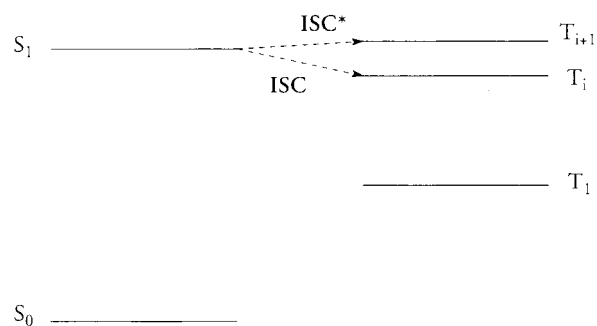


**Figure 7.** Schematic representation of the dominant channels for intersystem crossing in conjugated oligomers and polymers. ISC\* denotes an exothermic process, ISC an endothermic process.

singlet–triplet,  $S_1$ – $T_1$ , intersystem crossing. In all compounds we investigated, we find low-lying triplet excited states close to the lowest singlet excited state, that appear as better candidates for efficient ISC channels.

The spin–orbit couplings between the lowest singlet and the triplet excited states were computed by means of first-order perturbation theory. From simple symmetry arguments, we have pointed out the role of molecular disorder, in terms of twists of the aromatic rings along the conjugated path. While a vanishingly small SOC is obtained in all cases for the  $S_1$ – $T_1$  channel, interaction between  $S_1$  and higher-lying triplet states is more effective and leads to sizable expectation values for the spin–orbit Hamiltonian. We rationalize these results in terms of  $\sigma$ – $\pi$  mixing in the twisted structures. In oligothiophenes, the triplet wave functions giving rise to efficient spin–orbit coupling involve large contributions on the sulfur atoms, while the triple bonds of the ethynylene bridges are mostly responsible for the significant SOC values in oligo(phenylene ethynylene)s.

Using the golden-rule of radiationless transitions, we have estimated the intersystem crossing rates in a series of representative compounds. Although our approach does not allow us to provide quantitative results, it gives good insight into the likely mechanisms for intersystem crossing in conjugated polymers. As sketched in Figure 7, a few (mainly two) channels have been identified as the dominant contributions to the total ISC rate. These pathways involve triplet excited states that satisfy two criteria: (i) they are located close in energy to  $S_1$ , for significant overlap between the initial and final vibrational wave functions; and (ii) they display sizable spin–orbit coupling with the lowest singlet excited state. In most of the molecules we investigated, two triplet states fulfill these conditions, one located below  $S_1$  participating in the dominant exothermic channel and another lying just above  $S_1$  giving rise to an endothermic ISC route. Importantly, the magnitude of both types of channel has been calculated to decrease with oligomer size, as a result of smaller spin–orbit couplings and increased activation energies. It is remarkable that the same evolution has been obtained for the two types of conjugated structures we considered. Additional work is, however, needed to generalize further these observations.

As a reply to the questions raised in the Introduction section, we can propose two strategies for the engineering of efficient luminescent materials: One is to design highly delocalized conjugated structures with planar skeletons to reduce spin–orbit coupling and intersystem crossing. We note that luminescence quenching due to solid-state effects is also expected to be reduced in extended systems.<sup>12,38</sup>

The other is to take advantage of triplet emission in architectures including, either in the conjugated backbone or as substituents, heavy atoms to boost the spin–orbit couplings



and shorten the triplet radiative lifetime. Achievements of such work appear to be highly promising;<sup>39–41</sup> here, one can take benefit from the large yield of triplet excitons generated in LEDs upon charge injection and recombination.

**Acknowledgment.** The work in Mons is partly supported by the Belgian Federal Government “InterUniversity Attraction Pole in Supramolecular Chemistry and Catalysis (PAI 4/11)”, the European Commission (Brite-Euram contract BRPR-CT97-0469 “OSCA”), and the Belgian National Fund for Scientific Research (FNRS-FRFC). The work at Arizona is partly supported by the National Science Foundation (CHE-0078819). D.B. is a research fellow of the Belgian National Fund for Scientific Research (FNRS).

## References and Notes

- Burroughes, J. H.; Bradley, D. D. C.; Brown, A. R.; Marks, R. N.; Mackay, K.; Friend, R. H.; Burn, P. L.; Holmes, A. B. *Nature* **1990**, *347*, 539.
- See, for instance, *Primary Photoexcitations in Conjugated Polymers: Molecular Exciton versus Semiconductor Band Model*; Sariciftci, N. S., Ed.; World Scientific: Singapore, 1997.
- Becker, H.; Burns, S. E.; Friend, R. H. *Phys. Rev. B* **1997**, *56*, 1893.
- Cao, Y.; Parker, I. D.; Yu, G.; Zhang, C.; Heeger, A. J. *Nature* **1999**, *397*, 414.
- Ho, P. K. H.; Kim, J. S.; Burroughes, J. H.; Becker, H.; Li, S. F. Y.; Brown, T. M.; Cacialli, F.; Friend, R. H. *Nature* **2000**, *404*, 6777.
- Shuai, Z.; Beljonne, D.; Silbey, R. J.; Bredas, J. L. *Phys. Rev. Lett.* **2000**, *84*, 131.
- Kraabel, B.; Moses, D.; Heeger, A. J. *J. Chem. Phys.* **1995**, *103*, 5102.
- Rossi, R.; Ciofalo, M.; Carpita, A.; Ponterini, G. *J. Photochem. Photobiol. A: Chem.* **1993**, *70*, 59.
- Becker, R. S.; Seixas de Melo, J.; Macanita, A. L.; Elisei, F. *J. Phys. Chem.* **1996**, *100*, 18683. Becker, R.; Seixas de Melo, J.; Macanita, A. L.; F. E. *Pure Appl. Chem.* **1995**, *67*, 9.
- Paa, W.; Yang, J. P.; Helbig, M.; Hein, J.; Rentsch, S. *Chem. Phys. Lett.* **1998**, *292*, 607. Yang, J.-P.; Paa, W.; Rentsch, S. *Chem. Phys. Lett.* **2000**, *320*, 665.
- Pope, M.; Swenberg, C. E. *Electronic Processes in Organic Crystals*; Oxford University Press: New York, 1982.
- Cornil, J.; dos Santos, D. A.; Crispin, X.; Silbey, R.; Bredas, J. L. *J. Am. Chem. Soc.* **1998**, *120*, 1289.
- Woo, H. S.; Lhost, O.; Graham, S. C.; Bradley, D. D. C.; Friend, R. H.; Quattrocchi, C.; Bredas, J. L.; Schenk, R.; Müllen, K. *Synth. Met.* **1993**, *59*, 13.
- Wittmann, H. F.; Friend, R. H.; Kahn, M. S.; Lewis, J. *J. Chem. Phys.* **1994**, *101*, 2693. Beljonne, D.; Wittmann, H. F.; Köhler, A.; Graham, S.; Younus, M.; Lewis, J.; Raithby, P. R.; Khan, M. S.; Friend, R. H.; Bredas, J. L. *J. Chem. Phys.* **1996**, *105*, 3868.
- Dewar, M. J. S.; Zoebisch, E. G.; Healy, E. F.; Stewart, J. J. P. *J. Am. Chem. Soc.* **1995**, *107*, 3702.
- Dewar, M. J. S.; Thiel, W. *J. Am. Chem. Soc.* **1977**, *99*, 4899.
- Ridley, J.; Zerner, M. C. *Theor. Chim. Acta* **1973**, *32*, 111.
- Ohno, K.; *Theor. Chem. Acta* **1964**, *2*, 219. Klopman, G. *J. Am. Chem. Soc.* **1964**, *86*, 4550.
- Mataga, N.; Nishimoto, K. *Z. Phys. Chem.* **1957**, *13*, 140.
- Beljonne, D.; Cornil, J.; Friend, R. H.; Janssen, R. A. J.; Bredas, J. L. *J. Am. Chem. Soc.* **1996**, *118*, 6453.
- The Triplet State* Zahlan, A. B., Androes, G. M., Hameka, H. F., Heineken, F. M., Hutchison, C. A., Jr., Robinson, G. W., van der Waals, J. H., Eds.; Cambridge University Press: Cambridge, 1967. Lower, S. K.; El-Sayed, M. A. *Chem. Rev.* **1966**, *66*, 199.
- Newton, M. *Chem. Rev.* **1987**, *87*, 113.
- Marcus, R. A. *Rev. Mod. Phys.* **1993**, *65*, 599.
- Balzani, V.; Juris, A.; Venturi, M.; Campagna, S.; Serroni, S. *Chem. Rev.* **1996**, *96*, 759.
- Chawdhury, N.; Köhler, A.; Friend, R. H.; Wong, W. Y.; Lewis, J.; Younus, M.; Raithby, P. R.; Corcoran, T. C.; AlMandhary, M. R. A.; Khan, M. S. *J. Chem. Phys.* **1999**, *110*, 4963. Chawdhury, N.; Köhler, A.; Friend, R. H.; Younus, M.; Long, N. J.; Raithby, P. R.; Lewis, J. *Macromolecules* **1998**, *31*, 722.
- Beljonne, D.; Shuai, Z.; Friend, R. H.; Bredas, J. L. *J. Chem. Phys.* **1995**, *102*, 2042.
- Seixas de Melo, J.; Silva, L. M.; Arnaut, L. G.; Becker, R. S. *J. Chem. Phys.* **1999**, *111*, 5427.
- Osterbacka, R.; Wohlgenannt, M.; Vardeny, Z. V. *Phys. Rev. B* **1999**, *60*, 1253.
- Romanovskii, Y.; Fischer, A.; Scherf, U.; Personov, R.; Bassler, H. *Phys. Rev. Lett.* **2000**, *84*, 1027.
- Burin, A. L.; Ratner, M. A. *J. Chem. Phys.* **1998**, *109*, 6092.
- Theander, M.; Inganäs, O.; Mammo, W.; Olinga, T.; Svensson, M.; Andersson, M. R. *J. Phys. Chem. B* **1999**, *103*, 7771.
- Lanzani, G.; Nisoli, M.; Tubino, R. *Synth. Met.* **1996**, *76*, 39.
- Stampfl, J.; Tasch, S.; Leising, G.; Scherf, U. *Synth. Met.* **1995**, *71*, 2125.
- Xu, B.; Holdcroft, S. *J. Am. Chem. Soc.* **1993**, *115*, 8447.
- McClure, D. *J. Chem. Phys.* **1952**, *20*, 682. El-Sayed, M. *J. Chem. Phys.* **1963**, *38*, 2834.
- Krishna, V.; Goodman, L. *J. Chem. Phys.* **1962**, *37*, 912.
- Chosrovian, H.; Rentsch, S.; Grebner, D.; Dahm, D. U.; Birkner, E.; Naarmann, N. *Synth. Met.* **1993**, *60*, 23.
- Beljonne, D.; Cornil, J.; Silbey, R.; Bredas, J. L. *J. Chem. Phys.* **2000**, *112*, 4749. Muccini, M.; Schneider, M.; Taliani, C.; Sokolowski, M.; Umbach, E.; Beljonne, D.; Cornil, J.; Bredas, J. L. *Phys. Rev. B* **2000**, *62*, 6296.
- Baldo, M. A.; O'Brien, D. F.; You, Y.; Shoustikov, A.; Sibley, S.; Thompson, M. E.; Forrest, S. R. *Nature* **1998**, *395*, 151.
- Baldo, M. A.; Thompson, M. E.; Forrest, S. R. *Nature* **2000**, *403*, 6771.
- Cleave, V.; Yahioglu, G.; Le Barny, P.; Friend, R. H.; Tessler, N. *Adv. Mater.* **1998**, *11*, 285.